Synthesis, Characterization, and Highly Efficient Catalytic Reactivity of Suspended Palladium Nanoparticles

Chang-Bing Hwang, Yaw-Shyan Fu, Yi-Ling Lu, Shu-Wen Jang, Pi-Tai Chou,
C. R. Chris Wang, and Shuchun Joyce Yu[1]

Department of Chemistry, National Chung Cheng University, Ming Hsiung, Chia Yi, Taiwan 621

The catalytic activities of suspended nano-sized palladium catalysts toward various olefin hydrogenation reactions are reported. The Pd nanoparticles were prepared by a laser ablation method followed by careful characterization. Two types of Pd nanoparticle systems were fabricated and subjected to a series of catalytic activity measurements: (i) Pd nanoparticles stabilized by tetraoctylammonium bromide (TC$_8$ABr) ionic micelles with an average diameter of 2.4 ± 0.5 nm and (ii) bare-Pd nanoparticles with an average size of 12.7 ± 5.7 nm in diameter. The catalytic activities of both TC$_8$ABr–Pd and bare-Pd nanoparticles were examined by measuring their turnover numbers (TON) in several target olefin hydrogenation reactions, such as the transformations of styrene to ethylbenezene, 2-methyl-2-butene to 2-methylbutane, 1-octene to *n*-octane, *trans*-stilbene to bibenzyl, and cyclohexene to cyclohexane. Data are compared to the hydrogenation results using a commercially available Pd/C catalyst system under similar reaction conditions. An exclusive selectivity of the catalytic styrene hydrogenation reaction on the C=C bond, rather than on the aromatic ring, was found among three systems, giving ethylbenzene as the only product. The catalyst stability was found to be on the order of TC$_8$ABr–Pd $>$ bare-Pd $>$ 10% Pd/C.   © 2000 Academic Press

Key Words: palladium nanoparticles; olefin hydrogenation; catalyst.

INTRODUCTION

The quantum size effect associated with nanoscale particles has been intensively studied during the past 2 decades. Nanoparticles with properties between bulk materials and molecules are potentially useful for the new generations of chemical, optical, magnetic, and electronic devices (1, 2). In addition, their feasible application in the field of catalysis has received considerable attention (3–5). Consequently, a wide range of synthetic approaches regarding the preparation of metal nanoparticles in various matrices, including reduction method (6), sol–gel process (7), solvent evaporation of hydrophobic colloids (8), cross-linking in colloidal

aggregates (9), templates-directed methods (3d, 10), and bacterial superstructures (11), has been reported. We describe here an alternative synthetic route to prepare bare-Pd nanoparticle aggregates and surfactant-stabilized Pd nanoparticles using the laser ablation method (12) and the application of these Pd nanoparticles as potent hydrogenation catalysts for a series of olefins. In fact, the catalytic potential of noble-metal nanoparticles was first reported by Schmid (13) using Rh$_{55}$ clusters. However, the liability of Rh$_{55}$ clusters in solution did not allow any conclusive suggestion regarding its feasible application. The specific catalytic properties of nano-sized metal clusters are usually associated with a change in their electron properties relative to the bulk samples. This change is requisitioned by the quantum size effect and is usually prevailing with a great enhancement in catalytic activity (3–5). Recently, Pd nanoparticles protected by either micelles or organic polymers have been demonstrated to catalytically hydrogenate pyrene (14) and a selective double bond of dienes (15). In the present study, suspensions of Pd nanoparticles in ethyl acetate were prepared by a laser ablation method. The UV–Vis, EDX, and AA spectroscopic analyses and TEM image were used to characterize the palladium nanoparticles. The highly efficient activity of these nano-sized palladium catalysts were discussed within the framework of their catalytic performance in the olefin hydrogenation reactions.

EXPERIMENTAL

Catalyst Preparation

The laser ablation method was employed to fabricate both bare-Pd nanoparticles and TC$_8$ABr–stabilized Pd nanoparticles suspensions. A Pd metal plate was first cleaned by a regular cleaning procedure, which incorporates an ultrasonication by immersing the Pd plate into acetone and then dried ethyl acetate in sequence. While it is needed, fine sandpaper was employed to polish the surface before the ultrasonication. The Pd metal plate after regular cleaning was then fixed onto a Teflon disc placed at the

bottom of a glass vessel. A typical 3 ml of dried ethyl acetate solution was then added into the glass vessel. In the case of preparing the TC$_8$ABr–stabilized Pd nanoparticles suspension, 3 ml of 0.01 M tetraoctylammonium bromide (TC$_8$ABr) in the ethylacetate solution was employed at this stage. The TC$_8$ABr was used to form a micellar system, which serves as the stabilizers for the Pd nanoparticles. The ablation was then conducted by irradiating an unfocused Nd: YAG laser beam (2nd harmonic, 532 nm and 10 Hz, Continuum Model Surlite II) from the top onto the Pd metal plate perpendicularly. The laser power of 3.2 W, corresponding to the fluence of 8.6×10^{17} photons/pulse/cm^2, was employed throughout the study. The laser beam is ca. 6 mm in diameter and the pulse duration is 6 ns. The ablation time was typically set to 3 min. The suspended Pd nanoparticles formed during the ablation were then ready for the material characterization and catalytic studies. 10% Pd/C (Pd supported on the activated carbon) was purchased from Lancaster and used without further treatment prior to the catalytic activity measurements.

Catalyst Characterization

UV–Vis spectroscopy. The absorption spectra were recorded on a HP 8453 photodiode array spectrophotometer. The UV–Vis spectra of both bare- and TC$_8$ABr–Pd nanoparticles exhibit similar absorption spectral features, which are consistent with the electrostatic model prediction (16) on the collective dipolar oscillation (the surface plasmon) of free electrons of the Pd nanoparticles. The resonance of the surface plasmon for Pd nanoparticles suspended in water is predicted to be located at ca. 210 nm. To avoid the spectral cut-off region due to the absorption of ethyl acetate, the long-wavelength side of the surface plasmon band can be used routinely to roughly check the concentration of the Pd nanoparticles and the correctness of the experimental conditions.

Transmission electron microscope (TEM) and energy-dispersive X-ray (EDS). The size distributions of thus prepared Pd nanoparticles were determined from the TEM (JEOL JEM-1200EX) measurements. The TEM images for both TC$_8$ABr–Pd and bare-Pd nanoparticles are shown in Fig. 1. The size of TC$_8$ABr–Pd nanoparticles ($\sim 2.4 \pm 0.5$ nm in diameter, Fig. 1A) is more as evenly distributed as that of bare-Pd nanoparticles ($\sim 12.7 \pm 5.7$ nm in diameter, Fig. 1B). The results can be best rationalized by the micellar stabilization effect, which prevents Pd particles from self aggregation. As a result, the TC$_8$ABr–Pd nanoparticles system shows much smaller and higher uniformity in sizes. EDS analyses on individual Pd nanoparticles indicate that no detectable oxygen and other metallic impurities were present in the suspended Pd nanoparticles.

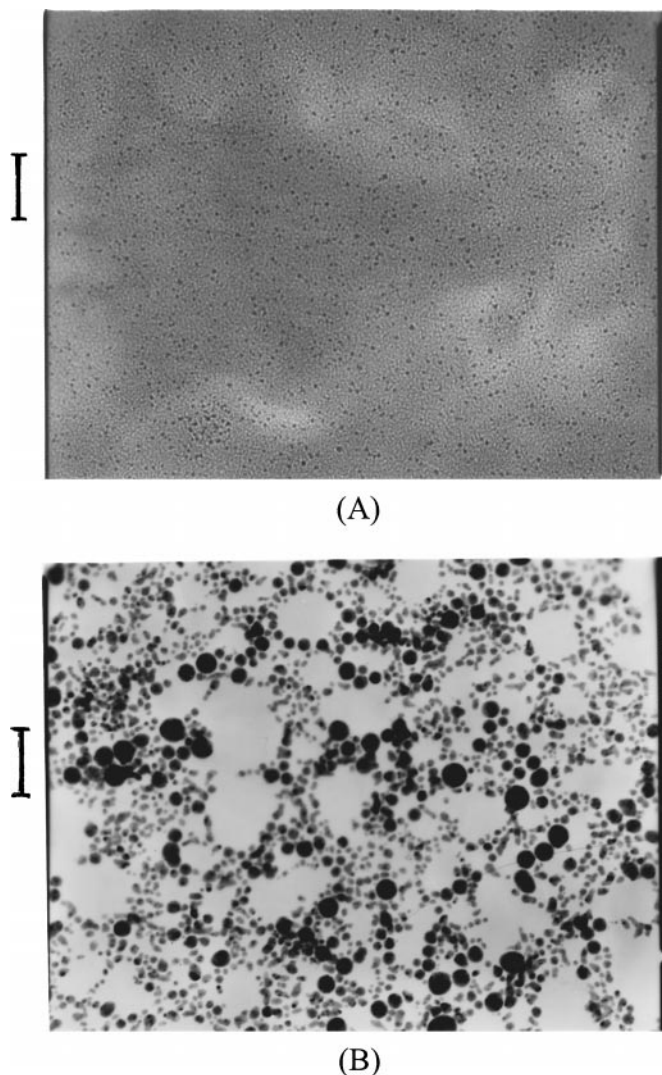*Atomic absorption (AA).* The weight percentages of Pd in the Pd/ethyl acetate suspensions were quantified by

(A)

(B)

FIG. 1. TEM image of (A) TC$_8$ABr–Pd nanoparticles. Scale bar = 50 nm; (B) bare-Pd nanoparticles. Scale bar = 100 nm.

atomic absorption (AA) (Perkin-Elmer model 3110) analyses. The AA analysis was conducted in parallel with the catalytic measurement for every freshly prepared Pd nanoparticle suspension. The content of Pd obtained from a typical preparation condition is ca. 20 μg in 3 ml of ethyl acetate.

Olefin hydrogenation and catalytic activity measurements. Catalytic olefin hydrogenation reactions were carried out under various H$_2$ gas pressures in a Parr high-pressure minireactor (Model 4560 series) at ambient temperature. A representative procedure for catalytic styrene hydrogenation reaction follows: To a glass sample vial was added 3 ml of a dry ethyl acetate suspension containing either the 10% Pd/C (5 mg) or one of the TC$_8$ABr–stabilized Pd nanoparticles and bare-Pd nanoparticles. To this solution was then transferred 0.3 ml of styrene (2.6 mmol). The reactor was flushed with H$_2$ gas before being charged with

H_2 gas pressures. The reaction mixture was then allowed to stir at ambient temperature. After 1-h reaction time, the H_2 gas was gradually discharged and the resulting mixture was subjected to ^{1}H NMR and gas chromatography analyses. NMR spectra were recorded on a Varian Gemini-200 or on a Bruker AMX 400 QNP spectrometer, and chemical shifts were reported relatively to TMS for ^{1}H NMR spectra in $CDCL_3$. Gas chromatography (GC) analyses were conducted on a Shimadzu GC-14B spectrometer. The gross turnover number (gross-TON) is taken into account as the relative catalytic activity, which is defined as moles of hydrogenation product produced per mole of palladium per hour at ambient temperature. For further detailed discussion, the gross-TON has been normalized by the estimated total catalyst surface area to give a specific turnover number (specific-TON), which is defined by the number of product molecules produced per square nanometer of Pd catalyst per hour. The product indentification and quantification (e.g., percentage of conversion) were determined by NMR and GC spectroscopic analyses, respectively.

RESULTS AND DISCUSSION

Table 1 shows the results of various olefin hydrogenation reactions catalyzed by TC_8ABr–Pd nanoparticles at ambient temperature. The commercially available Pd/C is often used as a catalyst for the hydrogenation of unsaturated organic molecules (17). In a comparative study, the control experiments were performed at various H_2 gas pressures containing 5 mg of 10% Pd/C at similar reaction conditions. The results listed in Table 1 indicate that values of gross-TON obtained from TC_8ABr–Pd nanoparticles were significantly higher than those obtained from 10% Pd/C. At a low H_2 gas pressure of 100 psi, TC_8ABr–Pd nanoparticles were found to be much more reactive than 10% Pd/C toward bulkier

linear olefins. The gross-TON ratios of TC_8ABr–Pd versus 10% Pd/C were measured to be 34 : 1 for styrene (entry 1), 44 : 1 for *trans*-stilbene (entry 4), and 25 : 1 for 1-octene (entry 3). For the case of cyclic olefin such as cyclohexene, the relative reactivity of TC_8ABr–Pd is ~20-fold as high as that of 10% Pd/C (entry 5). Apparently, the catalytic activity in both systems decreases as the steric bulk increases on the olefin substituents. For the case of the *tri*substituted olefin such as 2-methyl-2-butene, the hydrogenation has to be performed at an H_2 gas pressure as high as 800 psi to obtain a gross-TON value comparable to that of styrene (entries 1 and 2).

Table 2 summarizes the results of styrene hydrogenation promoted by three different catalyst systems, TC_8ABr–Pd nanoparticles, bare-Pd nanoparticles, and 10% Pd/C. The selectivity in converting styrene to ethylbenzene was demonstrated by the lack of detecting any ethylcyclohexane in all three systems using GC and/or ^{1}H NMR spectroscopic analyses. At an H_2 gas pressure of 100 psi, partial styrene conversions were observed in all three systems, affording the gross-TON values of 8167, 3511, and 238 (styrene mol/(Pd mol h), with an error percentage of <5%) for TC_8ABr–Pd nanoparticles, bare-Pd nanoparticles, and 10% Pd/C, respectively. The catalytic activity increased with an increase of the H_2 gas pressure for all three systems. At an H_2 gas pressure of 600 psi, an approximate unity styrene conversion was attained for both TC_8ABr–Pd, and bare-Pd nanoparticle catalyst systems (entries 1 and 3), while ca. 97% styrene conversion with a gross-TON value of 537 was observed by using 10% Pd/C catalyst (entry 2). When the H_2 gas pressure was lowered from 100 to 50 psi, a drop of ~5% in relative catalytic activity was observed for the TC_8ABr–Pd system (entry 1, the gross-TON value changed from 8167 to 7769). Under similar reaction conditions, however, a noticeable drop of 32% in catalytic

TABLE 1

Olefin Hydrogenation[a] over TC_8ABr–Stabilized Palladium Nanoparticles[b] and 10% Pd/C Catalyst[c]

			For TC_8ABr–Pd			For 10% Pd/C			
Entry	Substrate (mmol)	H_2 (psi)	gross-TON[d]	specific-TON[e]	%conver.[f]	gross-TON[d]	specific-TON[e]	%conver.[f]	Product[g]
1	Styrene (2.6)	100	8167	4.4×10^5	62	238	2.7×10^4	43	Ethylbenzene
2	2-Methyl-2-butene (2.8)	800	7803	4.2×10^5	55	524	7.0×10^4	88	2-Methylbutane
3	1-Octene (0.6)	100	3128	1.7×10^5	98	125	1.9×10^4	98	*n*-Octane
4	*trans*-Stilbene (1.0)	100	2418	1.3×10^5	50	55	8.7×10^3	26	Bibenzyl
5	Cyclohexene (0.5)	100	2048	1.1×10^5	77	104	1.2×10^4	98	Cyclohexane

[a] Reaction conditions: mmol of substrate are given in the table; 3 ml of ethyl acetate solvent; ambient temperature; 1-h reaction time.

[b] 0.01 M tetraoctylammonium bromide (TC_8ABr) surfactant; catalyst loading was quantified by AA spectroscopy to give 21 μg (entry 1), 21 μg (entry 2), 20 μg (entry 3), 22 μg (entry 4), and 20 μg (entry 5).

[c] Catalyst loading: 5 mg for entries 1–5.

[d] Gross-TON is defined as moles of product produced per mole of palladium per hour.

[e] Specific-TON is defined as the number of product molecules produced per square nanometer of Pd per hour.

[f] % conversion is determined by GC.

[g] Products were identified by both GC and NMR spectroscopies.

TABLE 2

Styrene Hydrogenation over Three Different Palladium Catalyst Systems[a]

Entry	Catalyst	Pd loading (μg)[c]	600 psi H_2		100 psi H_2		50 psi H_2		Product[f]
			Gross-TON	Specific-TON	Gross-TON	Specific-TON	Gross-TON	Specific-TON	
1	TC_8ABr–Pd[b]	21[c]	NA[d]	NA[d]	8167	4.4×10^5	7769	4.2×10^5	Ethylbenzene
2	10% Pd/C	500	537	6.1×10^4	238	2.7×10^4	163	1.8×10^4	Ethylbenzene
3	bare-Pd	26[c]	NA[d]	NA[d]	3511	7.7×10^5	ND[e]	ND[e]	Ethylbenzene

[a] Reaction conditions: 3 ml of ethyl acetate solvent; ambient temperature; 1-h reaction time.
[b] 0.01 M tetraoctylammonium bromide (TC_8ABr) surfactant.
[c] Catalyst loading was quantified by AA spectroscopy.
[d] NA = not available, 100% conversion of styrene to ethylbenzene was observed.
[e] ND = not determined, the experiment was not performed.
[f] Ethylbenzene was the only detectable product and was identified by both GC and NMR spectroscopies.

activity was measured for the 10% Pd/C system (entry 2, the gross-TON value changed from 238 to 163).

As stated above, TC_8ABr–Pd nanoparticles were demonstrated to be a relatively more reactive catalyst system in terms of gross-TON values when compared with bare-Pd nanoparticles. Theoretically, the overall surface areas of nonsupported metal catalysts are limited by the size of the catalyst particles. The fractions of surface atoms were estimated to be 40 and 7.5% for TC_8ABr–Pd (2.4 nm in diameter) and bare-Pd nanoparticles (12.7 nm in diameter), respectively. Also, the total surface areas for both systems, TC_8ABr–Pd and bare-Pd, used for catalytic studies can be estimated based on (i) TEM to determine the averaged particle diameters, (ii) AA to extract the concentrations of Pd atoms, and (iii) the roughly calculated number of atoms in each Pd particle. Accordingly, the total surface areas exposed to the reactants in the typical 3-ml sample suspensions for the TC_8ABr–Pd nanoparticles are estimated to be ca. 4.5 times larger than that of the bare-Pd nanoparticles. Therefore, the TC_8ABr–Pd nanoparticles are capable of providing greater catalyst surface area and facile H_2/styrene adsorption to afford higher TON values. However, the accessibility of the reactant to the Pd surface is also known to be limited by the presence of surfactant aggregates. Furthermore, the aggregation of bare-Pd nanoparticles might lead to the deactivation of their catalytic property. At this stage, each individual parameter unfortunately cannot be singled out; however, it is believed that the overall catalytic activity of the TC_8ABr–Pd system should result from the combination of the aforementioned effects.

In general, the relative catalytic activity (i.e., gross-TON) of nano-sized Pd particles with or without surfactant protection was found to be higher than that of 10% Pd/C by a factor of 40 and 20, respectively. However, differences in the relative catalytic activities between Pd nanoparticles and 10% Pd/C might have to be further rationalized by the results of surface area, size effect, structures sensitivity, and/or support dependency (14, 18). Therefore, an attempt

has been made to take into account of the contributions of the surface areas of Pd alone in three catalyst systems from the reported gross-TONs, namely, the specific-TON (see the Experimental section for the definition). We realized that the associated catalytic mechanisms may well be different and the correction is simply to the first-order approximation. The total surface area can be calculated by knowing the estimated number and size of particles participating in the reaction. It is directly related to the number of Pd atoms per particle, n, which is roughly estimated by $n = (r/r_0)^3$, where r_0 is the atomic radius of Pd and r is the radius of the Pd nanoparticles. The average radius of the particles has been determined directly by TEM images and/or XRD analyses. As a result, values of specific-TON for the hydrogenation of styrene were estimated to be ca. 4.4×10^5 for the case of the TC_8ABr–Pd catalyst (see entry 1, Table 1). For the 10% Pd/C system, which is a product with Pd nanoparticles supported on the activated carbon carrier, both TEM and XRD analyses were conducted to give an average size of Pd particle of 5 nm in diameter. By using 10% Pd/C as catalysts, the values of specific-TON corresponding to the same reaction were estimated to be 2.7×10^4 (19), which is a factor of 16 less than that of the TC_8ABr–Pd catalyst. Similarly, the normalized catalytic activities after surface area correction (i.e., specific-TON) for TC_8ABr–stabilized Pd nanoparticles are still higher than that of 10% Pd/C by a factor of 6, 9, 15, and 9 for the other four types of hydrogenation reactions listed in Table 1 (entries 2 to 5). The results indicate that excluding the surface area effect, other parameters such as particle size (quantum effect), surface structure, shape, etc., of the nanoparticles also play key roles in determining the catalytic property of the Pd nanoparticles. Further support can be given by the comparative catalytic property between two types of laser-ablated Pd nanoparticles. The specific-TON of the bare-Pd system is found to be ca. 2-fold higher (calculated from the data in Table 2) than that for the TC_8ABr–Pd system on styrene hydrogenation, which simply manifests the influence of
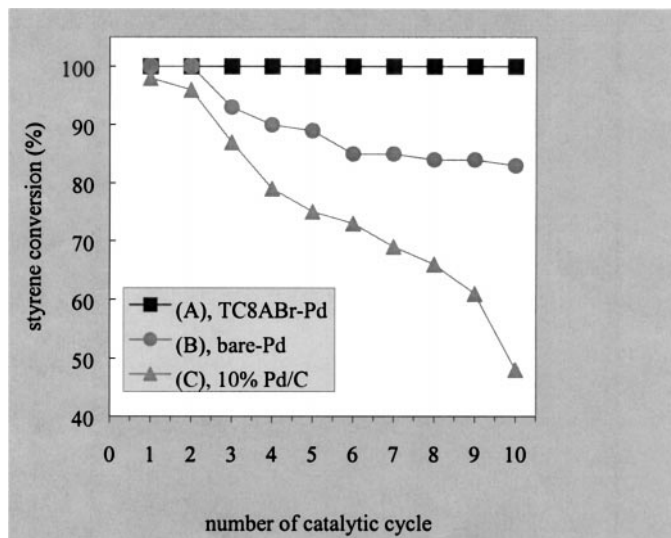
FIG. 2. The degree of catalyst deactivation throughout 10 continuous styrene hydrogenation cycles. Each reaction cycle is set to 1-h reaction time. (A) TC$_8$ABr–Pd nanoparticle catalyst; (B) bare-Pd nanoparticle catalyst; (C) 10% Pd/C catalyst.

the surfactant molecules on the H$_2$/olefin adsorption and possible size and structural effects. The size- and structure-dependent catalytic activities for both supported and non-supported metal nanoparticles have been reported in the literature. For example, a significant increase in pyrene hydrogenation activity with a decrease in size of palladium colloids has been demonstrated (14). Also, a pronounced structure sensitivity of catalytic CO oxidation on Au clusters supported on TiO$_2$ has also been discussed (3b).

A series of cyclic styrene hydrogenation reactions were performed to study the relative degree of deactivation upon catalysis. Figure 2 shows the results of catalyst deactivation in terms of the decrease in styrene conversion during 10 continuous hydrogenation cycles among three systems. At an H$_2$ gas pressure of 600 psi, TC$_8$ABr–Pd nanoparticles exhibit the greatest catalyst stability with ∼100% styrene conversion throughout 10 continuous cycles. Also, the TEM image of TC$_8$ABr–Pd nanoparticles after 10 hydrogenation cycles showed negligible difference from those freshly prepared by the laser ablation, suggesting that neither significant particle aggregation nor decomposition occurred during the course of hydrogenation. Conversely, the bare-Pd system underwent 17% deactivation (styrene conversion dropped from 100 to 83%) presumably due to a certain degree of particle aggregation. The 10% Pd/C, however, deactivated the most under the same conditions, in which the styrene conversion dropped from 98 to 48%.

CONCLUSION

In summary, various types of nano-sized Pd catalysts can be easily prepared by the laser ablation method. Smaller Pd particle sizes were obtained with the use of TC$_8$ABr surfactant to prevent aggregation as compared to that of the bare-Pd system. Both TC$_8$ABr–Pd and bare-Pd nanoparticles are proven to be powerful olefin hydrogenation catalysts over commercially available 10% Pd/C. Although surface areas should be considered to be one factor, other factors such as particle size, surface structure, etc., of the nanoparticles also play key roles to account for the indisputable differences in their relative catalytic properties toward various olefin hydrogenation. Three catalyst systems investigated in the present study exhibit different catalyst stability, which is on the order of TC$_8$ABr–Pd > bare-Pd > 10% Pd/C. More insights into the study of size- and structure-dependant catalytic properties are currently in progress.

REFERENCES

1. (a) Marinakos, S. M., Shultz, D. A., and Feldheim, D. L., *Adv. Mater.* **11**, 134 (1999). (b) Brousseau, L. C., III, Zhao, Q., Shultz, D. A., and Feldheim, D. L., *J. Am. Chem. Soc.* **120**, 7645 (1998). (c) Feldheim, D. L., and Keating, C. D., *Chem. Soc. Rev.* **27**, 1 (1998). (d) Alvarez, M. M., Khoury, J. T., Schaaff, T. G., Shafigullin, M. N., Vezmar, I., and Whetten, R. L., *J. Phys. Chem. B* **101**, 3706 (1997). (e) Feilchenfeld, H., Chumanov, G., and Cotton, T. M., *J. Phys. Chem.* **100**, 4937 (1996). (f) Chumanov, G., Sokolov, K., Gregory, B., and Cotton, T. M., *J. Phys. Chem.* **99**, 9466 (1995).
2. (a) Andres, R. P., Bein, T., Dorogi, M., Feng, S., Henderson, J. I., Kubiak, C. P., Mahoney, W., Osifchin, R. G., and Reifenberger, R., *Science* **272**, 1323 (1996). (b) Peschel, S., and Schmid, G., *Angew. Chem. Int. Ed. Engl.* **34**, 1442 (1995). (c) Bradley, J. S., "Clusters and Colloids" (G. Schmid, Ed.), Chapter 6. VCH, Weinheim 1994. (d) Colvin, V. L., Goldstein, A. N., and Alivisatos, A. P., *J. Am. Chem. Soc.* **114**, 5221 (1992).
3. (a) Zhao, M., and Crooks, R. M., *Adv. Mater.* **111**, 217 (1999). (b) Valden, M., Lai, X., and Goodman, D. W., *Science* **281**, 1647 (1998). (c) Reddington, E., Sapienza, A., Gurau, B., Viswanathan, R., Sarangapani, S., Smotkin, E. S., and Mallouk, T. E., *Science* **280**, 1735 (1998). (d) Che, G. L., Lakshmi, B. B., Fisher, E. R., and Martin, C. R., *Nature* **393**, 346 (1998).
4. (a) Rainer, D. R., Xu, C., and Goodman, D. W., *J. Mol. Catal. A: Chem.* **119**, 307 (1997). (b) Goodman, D. W., *J. Phys. Chem.* (Centennial Ed.) **100**, 13090 (1996). (c) Acres, G. J. K., and Hards, G. A., *Philos. Trans. R. Soc. London A* **354**, 1671 (1996). (d) Aiken, J. D., III, Lin, Y., and Finke, R. G., *J. Mol. Catal. A: Chem.* **114**, 29 (1996).
5. (a) Reetz, M. T., and Helbig, W., *J. Am. Chem. Soc.* **116**, 7401 (1994). (b) Lewis, L. N., *Chem. Rev.* **93**, 2693 (1993). (c) Schmid, G., *Chem. Rev.* **92**, 1709 (1992). (d) Pocard, N. L., Alsmeyer, D. C., McGreery, R. L., Neenan, T. X., and Callstrom, M. R., *J. Am. Chem. Soc.* **114**, 769 (1992).
6. A few examples for syntheses of Pd nanoparticles: (a) Chemical reduction: Teranishi, T., and Miyake, M., *Chem. Mater.* **10**, 594 (1998). (b) Sonochemical reduction: Okitsu, K., Mizukoshi, Y., Bandow, H., Yamanoto, T. A., Nagata, Y., and Maeda, Y., *J. Phys. Chem. B* **101**, 5470 (1997). (c) Electrochemical reduction: Reetz, M. T., Helbig, W., Quaiser, S. A., Stimming, U., Breuer, N., and Volgel, R., *Science* **267**, 367 (1995). (d) Chang, S. S., Shih, C. W., Chen, C. D., Lai, W. C., and Wang, C. R. C., *Langmuir* **15**, 701 (1999).

7. Li, T., Moon, J., Morrone, A. A., Mecholsky, J. J., Talham, D. R., and Adair, J. H., *Langmuir* **15**, 4328 (1999).

8. (a) Petit, C., Taleb, A., and Pileni, M.-P., *Adv. Mater.* **10**, 259 (1998). (b) Murray, C. B., Kagan, C. P., and Bawendi, M. G., *Science* **270**, 1335 (1995). (c) Vossmyer, T., Reck, G., Katsikas, L., Haupt, E. T. K., Schultz, B., and Weller, H., *Science* **267**, 1476 (1995).

9. (a) Brousseau, L. C., III, Novak, J. P., Marinakos, S. M., and Feldheim, D. L., *Adv. Mater.* **11**, 447 (1999). (b) Korgel, B. A., and Fitzmaurice, D., *Adv. Mater.* **10**, 661 (1998). (c) Andres, R. P., Bielefeld, J. D., Henderson, J. I., Janes, D. B, Kolagunta, V. R., Kubiak, C. P., Mahoney, W., Osifchin, R. G., and Reifenberger, R., *Science* **273**, 1690 (1996). (d) Brust, M., Bethell, D., Schiffrin, D. J., and Kiely, C. J., *Adv. Mater.* **7**, 795 (1995).

10. (a) Martin, C. R., *Science* **266**, 1961 (1994). (b) Petit, C., Lixon, P., and Pileni, M., *J. Phys. Chem.* **97**, 12974 (1993). (c) Murray, C. B., Norris, D. J., and Bawendi, M. G., *J. Am. Chem. Soc.* **115**, 8706 (1993). (d) Zhang, Y., Raman, N., Bailey, J. K., Brinker, C. J., and Crooks, R. M., *J. Phys. Chem.* **96**, 9098 (1992). (e) Shenton, W., Pum, D., Sleytr, U. B., and Mann, S., *Nature* **389**, 585 (1997). (f) Dieluweit, S., Pum, D., and Sleytr, U. B., *Supramol. Sci.* **5**, 15 (1998). (g) Shenton, W., Davis, S. A., and Mann, S., *Adv. Mater.* **11**, 449 (1999).

11. Davis, S. A., Patel, H. M., Mayes, E. L., Mendelson, N. H., Franco, G., and Mann, S., *Chem. Mater.* **10**, 2516 (1998).

12. (a) Neddersen, J., Chumanov, G., and Cotton, T. M., *Appl. Spectrosc.* **47**, 1959 (1993). (b) Fojtik, A., and Henglein, A., *Ber. Bunsen-Ges. Phys. Chem.* **97**, 252 (1993). (c) Wu, K. T., Yao, Y. D., Wang, C. R. C., Chen, P. F., and Yeh, E. T., *J. Appl. Phys.* **85**, 5959 (1999). (d) Chen, C. D., Yeh, Y. T., Chou, P. T., and Wang, C. R. C., in preparation.

13. Schmid, G., *Aspects Homogeneous Catal.* **7**, 1 (1990).

14. Wilcoxon, J. P., Martino, A., Baughmann, R. L., Klavetter, E., and Sylwester, A. P., *Mater. Res. Soc. Symp. Proc.* **286**, 131 (1993).

15. Hirai, H., Yakura, N., Seta, Y., and Hodoshima, S., *React. Polym.* **37**, 121 (1998).

16. For example: Creighton, J. A., and Eadon, D. G., *J. Chem. Soc. Faraday Trans.* **87**, 3881 (1991), and our calculations were based on modified Mie/Drude formalism.

17. Siegel, S., "Comprehensive Organic Synthesis" (B. M. Trost and I. Fleming, Eds.), Vol. 8, pp. 417–442. Pergamon, Oxford, 1991.

18. (a) Boudart, M., *J. Mol. Catal.* **30**, 27 (1985). (b) Gates, B. C., *Chem. Rev.* **95**, 511 (1995). (c) Moiseev, I. I., *J. Organomet. Chem.* **488**, 183 (1995). (d) Follstaedt, D. M., *Appl. Phys. Lett.* **62**, 1116 (1993). (e) Eaglesham, D. J., White, A. E., Feldman, L. C., Moriya, N., and Jacobson, D. C., *Phys. Rev. Lett.* **70**, 1643 (1993). (f) Haruta, M., *Catal. Today* **36**, 153 (1997).

19. Specific-TON was obtained by assuming that the entire surface areas calculated for each Pd particle are available for the hydrogenation reaction. Note that the calculated specific-TON for the Pd/C system should be considered as a lower-limit number since a certain percentage of the surface atoms is occupied by the activated carbon carrier and only part of the surface atoms is exposed to the reactant molecules.